



**HAL**  
open science

## Three DOF Microrobotic platform based on capillary actuation.

Cyrille Lenders, Pierre Lambert, Michaël Gauthier

► **To cite this version:**

Cyrille Lenders, Pierre Lambert, Michaël Gauthier. Three DOF Microrobotic platform based on capillary actuation.. IEEE Transactions on Robotics, 2012, 28 (5), pp.1157-1161. 10.1109/TRO.2012.2199009 . hal-00798857

**HAL Id: hal-00798857**


**<https://hal.science/hal-00798857>**

Submitted on 11 Mar 2013

**HAL** is a multi-disciplinary open access archive for the deposit and dissemination of scientific research documents, whether they are published or not. The documents may come from teaching and research institutions in France or abroad, or from public or private research centers.

L'archive ouverte pluridisciplinaire **HAL**, est destinée au dépôt et à la diffusion de documents scientifiques de niveau recherche, publiés ou non, émanant des établissements d'enseignement et de recherche français ou étrangers, des laboratoires publics ou privés.

## Three DOF Microrobotic Platform Based on Capillary Actuation

Cyrille Lenders, Pierre Lambert, and Michaël Gauthier 

**Abstract**—This paper presents a new microrobotic platform actuated by capillary effects, combining surface tension and pressure effects. The device has 6 degrees of freedom (dof) among which three are actuated:  $z$  axis translation having a stroke of a few hundreds of microns, and  $\theta_x$  and  $\theta_y$  tilt up to about  $15^\circ$ . The platform is submerged in a liquid and placed on microbubbles whose shapes (e.g. height) are driven by fluidic parameters (pressure and volume). The modeling of this new type of compliant robot is described and compared to experimental measurements. This work paves the way for interesting actuation and robotic solution for submerged devices in the microscale.

**Index Terms**—Micro/Nano Robots, Manipulation and Compliant Assembly, Fluidic Actuators, Surface Tension.

### I. INTRODUCTION

Micro-assembly deals with the assembly of submillimetric components. The operations consisting of gripping, moving, placing and releasing microcomponents at defined locations have to deal with forces inherent to microworld. To minimize the effects of some of these forces that are difficult to control, a strategy consists in performing the manipulation in a liquid [10].

To achieve the objective of automated assembly of microcomponents, there is a need for new devices that will address the current problems of micro-assembly such as the lack of compliance of the structures, which, combined with positioning and manufacturing errors, can lead to the destruction of the components [20], [4].

Some authors have proposed to include compliance in the grippers [6], [12], [21], [23], but the drawback of such devices is the risk of oscillation when accelerating the gripper. Other authors have proposed to include compliance in the support table, based on the use of springs [4]. But these systems are generally bulky or fragile if a low stiffness is required. Besides, these systems cannot be easily actuated. We propose in this paper a novel compliant table to perform assembly operations, which is based on the use of surface tension effect of gaseous bridges (bubbles) between two solids in a liquid. Such table could be used as support for assembly operations, with a moving microgripper bringing new components and assembling them.

Using bubbles as actuation mean for microsystems has already been investigated, but their are generally based on the expansion or coalescence of bubbles [19], or their compliance are not taken into account [9].

The objective of this paper is to present the microbubble-based actuation system, a model to predict its behavior and finally to show the advantages of such system.

### II. DEVICE OVERVIEW

The device presented here is a compliant platform that can be used to perform microrobotic assembly tasks in liquid environment. The table has six degrees of freedom (DOF), among which three are actuated: the translation along the direction orthogonal to the platform plane ( $\bar{z}$ ), and two rotations along axes parallel to the platform plane.

The device is made out of three main components: the moving table, the three bubbles which are used as compliant actuators, and the platform from which the bubbles are generated (Fig. 1).

C. Lenders and P. Lambert are with Bio Electro and Mechanical Systems Department, Université libre de Bruxelles (U.L.B.), Av. F.D. Roosevelt 50, 1050 Bruxelles, Belgium (e-mail: clenders@ulb.ac.be, plambert@ulb.ac.be)

M. Gauthier and P. Lambert are with the FEMTO-ST Institute, UMR CNRS 6174 - UMR INSMM UTBM, AS2M Department, 24 rue Alain Savary, 25000 Besançon, France (e-mail: michael.gauthier@femto-st.fr, pierre.lambert@femto-st.fr).

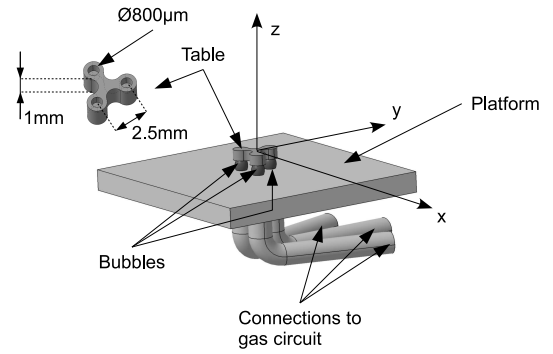


Fig. 1. Schematic view of the device, composed of a compliant table lying on 3 bubbles generated from a platform

Bubbles are the key of this device. Thanks to surface tension at the gas-liquid interface, and to the compressibility of the gas, a microbubble can be used as a compliant actuator. Indeed, the force developed by a bubble sandwiched between two solids has two components: one due to surface tension along the triple line (where solid, liquid and gas touch each other), and one due to the pressure gradient across the interface. If the contact angles in the liquid are smaller than  $90^\circ$ , the mean curvature of bubble interface is positive, and the pressure inside the bubble is larger than in the surrounding liquid. When the bubble is squeezed, the bubble is compressed and exerts a repulsive force on the solids. When the bubble is stretched, the bubble exerts an attractive force on the solids. Its behavior is comparable to a spring, from a mechanical point of view. But we will demonstrate that a bubble presents several advantages compared to classical mechanical springs. One of these advantages is that it is possible to actuate the bubbles using fluidic parameters ( $P, V$ ).

To be efficient, it is necessary to control the generation of the bubbles. An interesting way is to use a system derived from a syringe pump: the idea is to vary the volume of a tank containing gas in order to push the gas out of a hole. This principle has been developed in [15], in which it is underlined that surface tension must be taken into account in the bubble generator design. Some authors propose other principles for bubble generators, such as electrolysis [2], [3], [5], [16], [13], [22] or temperature rise [1], [7], [8], [12], [18], but the control of bubble size is more complex with these methods.

### III. DESIGN AND MANUFACTURING

When designing the device, the weight of the table should be considered, since it will use some of the bubble compliance to reach equilibrium. Consequently, the table has a trefoil shape (Fig.1) in order to reduce the weight of the platform.

But more important is the anchoring of the bubbles on the platform and on the table. The anchoring is a mean to ensure the bubbles will remain at a specific location even under mechanical stress. Two methods can be used to ensure this anchoring: a mechanical method and a chemical method [17]. In both cases, the idea is to create an energetic barrier preventing the triple line (where solid, liquid and gas phases meet) from moving. The mechanical method consists in creating a sudden variation in the solid part profile: the contact angle  $\theta$  (Fig. 4) must increase up to an angle called advancing angle value before the triple line can move. The chemical method consists in the deposition of a coating having a different surface energy. Here again, a movement of the triple line requires a change of the contact angle at the borderline of the two surfaces with different energy.

Another advantage for bubbles is that they induce the automatic centering of the table. Because of energy minimization, bubbles

tend to have the smallest possible interface surface. Henceforth, the bubbles will always move the table in such a way they are in the most favorable position. If the table and platform anchoring means have the same layout, the table will automatically center above the platform to superpose both layouts. The assembly of the table with the rest of the device is therefore very easy.

The presented prototype is made out of aluminum and has been manufactured using a conventional CNC milling machine. In this design, the anchoring has been realized using the mechanical method. Figure 2 (a) shows the anchoring in this first design. This method has the advantage of being very simple. However, there is a more efficient configuration, illustrated on Fig. 2 (b), but this configuration could not be manufactured using conventional machining processes. We have already started investigating to find other manufacturing means. One promising method is to use an excimer laser to machine polycarbonate.

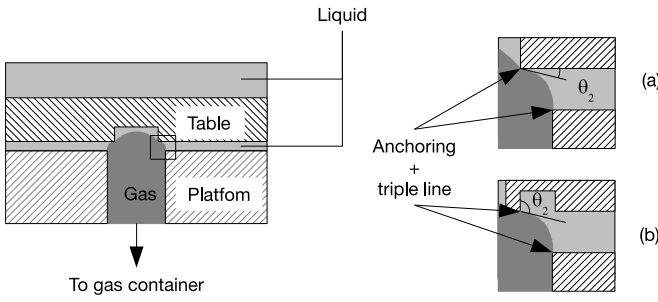


Fig. 2. Illustration of one leg of the table. A bubble is generated from the platform and lift the table. The anchoring means are in this case geometrical changes that improve the fixation of the line where solid-liquid and gas touches each other (triple line)

The bubble generator is based on a volume control, like a syringe pump. In the prototype, the bubble generator is a flexible hose containing the gas, which is squeezed to generate the bubble. The volume of gas initially contained in the hose can be adjusted by filling the hose with an incompressible fluid (Fig. 3).

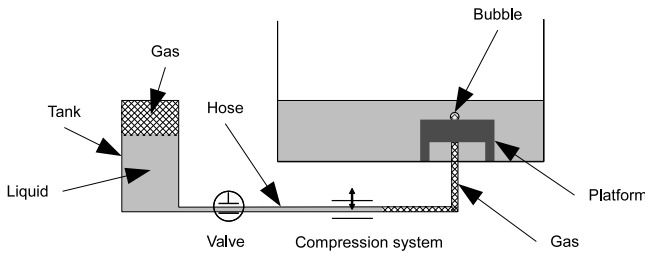


Fig. 3. Illustration of volume controlled bubble generator for the prototype. A bubble is grown by squeezing the flexible hose joining the platform and a container

#### IV. EQUATIONS

The ultimate purpose of this paper is to find the dynamic equation to predict the movement of the table under mechanical stress. We propose to model the dynamic of the table as a mass-spring-dashpot system. The general equations for actuated movements are:

$$m\ddot{h} + b_t\dot{h} + k_t h = F_{ext} \quad (1)$$

$$I_{x,y}\ddot{\alpha}_{x,y} + b_r\dot{\alpha}_{x,y} + k_r\alpha_{x,y} = \Gamma_{x,y} \quad (2)$$

where  $m$  is the mass of the table,  $h$  is the gap between the platform and the table,  $b_t$  is the viscous friction coefficient,  $k_t$  is the stiffness coefficient,  $F_{ext}$  is the force resultant component along the axis orthogonal to the platform ( $z$  axis),  $I_{x,y}$  is the moment of inertia along  $x$  and  $y$  axes,  $\alpha_{x,y}$  is the rotation angle in the direction  $x$  and  $y$ ,  $b_r$  is the viscous coefficient for rotation movement,  $k_r$  is the rotation stiffness coefficient, and  $\Gamma_{x,y}$  is the torque resultant along  $x$  and  $y$  direction.

In this paper, we will focus on the modeling of  $k_t$ . To determine the stiffness of the table, we have to determine the stiffness of one bubble. The total stiffness can be seen as the sum of the stiffness for each bubble, since the configuration is like three parallel springs.

To find the stiffness of a single bubble, we have to model the force developed by a bubble as a function of the distance between the table and the platform. This model takes account of the total volume in the bubble generator gas circuit  $V$ , the surface tension at the fluid-gas interface  $\gamma$ , the pressure in the liquid outside the bubble  $P_0$ , the temperature  $T$ , and the geometry of the anchoring means.

We suppose that the anchoring means are circular, and the table is placed above the platform in such a way that the bubbles have an axisymmetric shape.

Laplace law relates the surface tension  $\gamma$ , the pressure drop across the interface  $\Delta P$  (pressure inside bubble minus pressure outside bubble), and the mean curvature of the interface  $H$  (Fig.4):

$$\Delta P = 2\gamma H \quad (3)$$

If the height of the bubble is smaller than the capillary length (i.e. Bond number smaller than 1, meaning that gravity effects are lower than surface tension effects), the variation of hydrostatic pressure along  $z$  axis is negligible. Therefore, the mean curvature is uniform along  $z$  axis. The equation of interface profile  $r(z)$  (Fig. 4) is given by:

$$\frac{\Delta P}{\gamma} = 2H = -\frac{\frac{\partial^2 r}{\partial z^2}}{\left(1 + \left(\frac{\partial r}{\partial z}\right)^2\right)^{\frac{3}{2}}} + \frac{1}{r\left(1 + \left(\frac{\partial r}{\partial z}\right)^2\right)^{\frac{1}{2}}} \quad (4)$$

The boundary conditions for this ODE are given by the bubble anchoring means, which impose  $r$  at both ends of the profile. The value of the mean curvature is constrained by fluidic parameters. Indeed, Laplace equation (3) indicates that surface tension is responsible for a pressure drop across bubble interface. Since the bubble is compressible, the pressure variation in the bubble will be responsible for a volume change. Using the gas law ( $R_g$  is the gas constant), it is possible to determine the new gas volume in the system (bubble plus gas container):

$$(P_0 + \Delta P)V = nR_g T \quad (5)$$

The mean curvature  $H$  must be chosen so that (5) agrees with the number of mole  $n$  in the gas system. As a result there is a coupling between surface tension and gas compressibility.

When the interface geometry is found, it is possible to calculate the force generated by the bubble. As already mentioned, the force developed by a bubble has two components [11].

The surface tension force represents the tension in the interface. The force is the resultant of the distributed force tangent to the interface along the triple line. It is proportional to the sine of the contact angle, and to the surface tension:

$$\overline{F}_{TS} = \oint_{\text{Triple line}} \gamma \sin(\theta) dl \vec{z} = \pi s \gamma \sin(\theta) \vec{z} \quad (6)$$

where  $s$  is the diameter of the anchoring circle and:

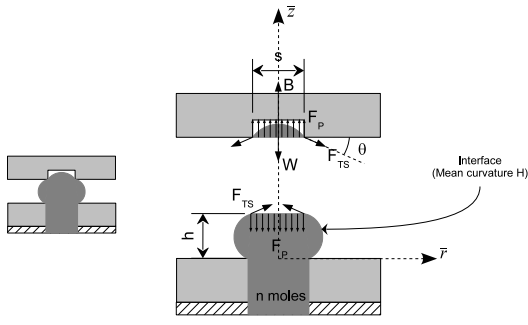


Fig. 4. Free body diagram of the system.  $h$  is the gap between the table and the platform.  $W$  and  $B$  are the weight and the buoyancy, respectively.  $s$  is the diameter of the pinning circle, the triple line. The capillary force has two components:  $F_{TS}$  is the surface tension contribution, which must be integrated along the triple line, and  $F_P$  is the pressure drop contribution, which must be integrated on the surface delimited by the triple line.

$$\cotan\theta = -\frac{\partial r}{\partial z} \quad (7)$$

The pressure force represents the effect of the pressure gradient across the bubble interface:

$$\overline{F_P} = \iint_{\text{Solid/gas interface}} \Delta P dS \vec{z} = \pi \frac{s^2}{4} \Delta P \vec{z} \quad (8)$$

The total vertical force  $\overline{F} = \overline{F_P} + \overline{F_{TS}}$  is therefore a function of the bubble shape and the surface tension  $\gamma$ . Bubble shape is given by its mean curvature  $H$  and the gap  $h$ . Together,  $H$  and  $h$  define a volume which is linked to the pressure by (3) and the number of gas mole  $n$  in the system. It is interesting to notice that these equations could be inverted, where the number of gas mole and the pressure should be sufficient to deduce the gap  $h$  and the force applied to the table  $F$  (Fig. 5). This is interesting because pressure measurement can be done anywhere in the gas circuit, avoiding the need for a position sensor to measure  $h$ .

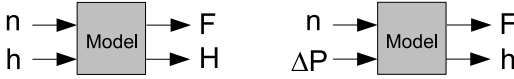


Fig. 5. Our model allows to find  $H$  and  $F$  assuming  $n$  and  $h$ . This model can be inverted to find  $F$  and  $h$  from the knowledge of  $n$  (known from setup configuration or calibration) and  $\Delta P$ , which may be measured anywhere in the circuit

The model detailed above was used to size up the prototype. We first defined the geometry of the anchoring circle. Then we assumed a bubble (known height) is generated from the platform. Based on these data, it is possible to define the distance between the table and the platform when they come into contact. When the table and the bubble make contact,  $\overline{F} = \vec{0}$ . From the model, we search for  $\overline{F}$  as a function of  $h$ . The iterative resolution scheme is shown in Fig. 6. We vary the distance  $h$  and we search for the interface mean curvature  $H$  ensuring a constant gas mole number  $n$ . When  $H$  is found for a value of the gap  $h$ , it is possible to calculate the force generated by the bubble. The derivative  $\partial \overline{F} / \partial h$  allows determining the stiffness of the bubble. Moreover, the model predicts that the volume of the gas circuit will have a significant influence on bubble stiffness.

In Fig. 7, the evolution of  $\overline{F}$  as a function of the gap distance  $h$  is drawn for configurations with a large gas tank and a small gas tank, leading to different stiffnesses. We have also indicated the results if the fluid was not compressible (constant volume). There is a distance

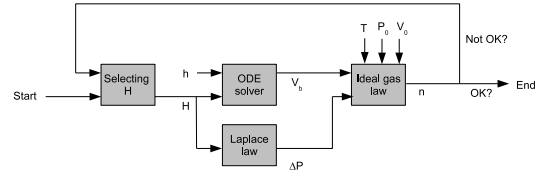


Fig. 6. To calculate the force applied by the bubble on the table, a first guess is made for the mean curvature of the bubble  $H$ . Together with the gap  $h$ , the profile of the bubble is calculated, from which the volume of the bubble  $V_b$  is inferred.  $H$  is also used to calculate the pressure drop  $\Delta P$  across bubble interface. The pressure and volume lead to the amount of gas moles  $n$ , which is supposed constant. In case  $n$  is not correct, the value  $H$  is adjusted and a new iteration is performed

at which the force is zero, which is the distance at which bubble and table come into contact. The shape of the bubble is at this point a portion of a sphere. If  $h$  increases, we see that the force is negative, pulling the table towards the platform, while if  $h$  decreases, the force is positive, pushing the table away from the platform.

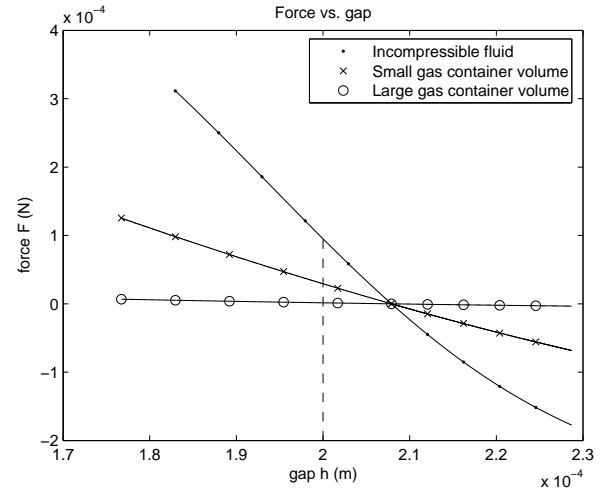


Fig. 7. Illustration of force vs. gap evolution for different gas system volume. The initial bubbles are the same for each simulation ( $s_{\text{bottom}} = 10^{-3}$  m,  $s_{\text{top}} = 0.8 \cdot 10^{-3}$  m,  $\gamma = 72 \cdot 10^{-3}$  N m $^{-1}$ ,  $P_0 = 101325$  Pa and bubble height before contact:  $0.4 \cdot 10^{-3}$  m). If the gas container is large (here  $10^{-6}$  m $^3$ ), a small variation of volume will not change pressure significantly, so the pressure variation and bubble curvature variations are small. The stiffness of the bubble is in this case small ( $0.2$  N m $^{-1}$  at  $h = 200$   $\mu$ m). On the contrary, if the gas system volume is small (here  $10^{-8}$  m $^3$ ), any volume variation will induce a significant change in the gas pressure, and the shape of the bubble will vary significantly. The stiffness of the bubble is therefore larger ( $3.9$  N m $^{-1}$  at  $h = 200$   $\mu$ m). We have also indicated the case of an incompressible fluid, for which the stiffness is even larger ( $12.6$  N m $^{-1}$  at  $h = 200$   $\mu$ m)

## V. EXPERIMENTAL RESULTS

The model has been validated experimentally using the prototype. We first present a demonstration of the use of the prototype. Then we will apply mechanical loads on the table and compare the stiffness to model predictions.

### A. Demonstration of the Prototype

We have manufactured and tested the prototype of the compliant table carried by bubbles. We have demonstrated that bubbles were able to withstand the force exerted by an aluminum table. We have also demonstrated that it is possible to tilt the table or to move it in the vertical direction, by controlling the amount of gas injected in

each bubble. The 3 actuated DOF are illustrated in Fig. 8. Finally, we have demonstrated that the table was compliant and able to move under an external solicitation (Fig. 9).

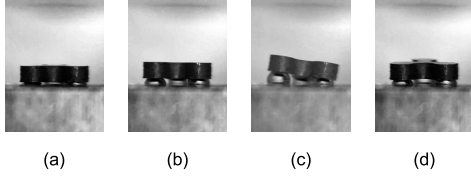


Fig. 8. View of the different degrees of freedom. (a) reference position, (b) vertical translation (here  $\approx 250\mu\text{m}$ ), (c,d) rotations (here  $\approx 10^\circ$ )

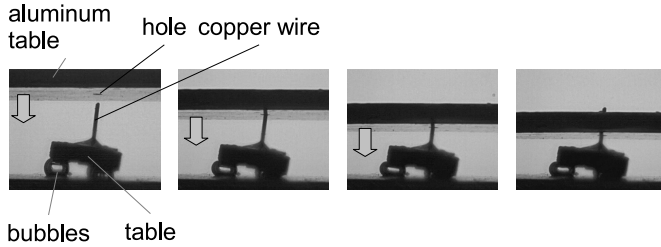


Fig. 9. Illustration of the table compliance. A  $200\mu\text{m}$  diameter copper wire has been glued on the table. An aluminum plate with a  $400\mu\text{m}$  diameter hole is moved down. Bubbles under the table change their shape in order to absorb the misalignment of the wire and the hole, preventing the deformation of the copper wire.

### B. Validation of Vertical Force Model

The model has been validated experimentally using the prototype. We used an image recording system to measure the gap, and we increased the force applied on the table by posing objects of known mass and density on the table (Fig. 10). Figure 11 shows the measurement points and the corresponding model curve. Each measurement has been repeated 5 times, inducing some dispersion on the gap measured. In order to best match the measurements by the model curve, we have assumed a linear diminution of  $n$  with the gap, i.e. with the experiment time, of at maximum 0.5%. This is justified by the gas dissolution in the liquid, and by the permeability of the flexible hoses used in the system.

We can conclude from these simulations that in these configurations, the vertical stiffness of a single bubble is between  $0.67\text{Nm}^{-1}$  and  $0.86\text{Nm}^{-1}$ . The stiffness of the entire table is 3 times this value.

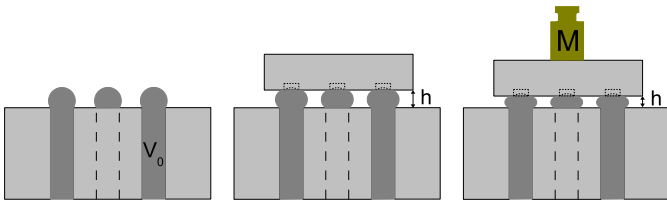


Fig. 10. Principle of the experimental validation of the vertical force model. First, bubbles are generated. Then the table is laid on the bubbles. The corresponding gap  $h$  is such that bubbles compensate the weight of the table, minus buoyancy. Finally other masses are added on the table and the evolution of  $h$  is measured)

## VI. CONCLUSION AND PERSPECTIVES

We have presented in this paper a new design of compliant table, using the properties of gaseous bridges (bubbles) as compliant

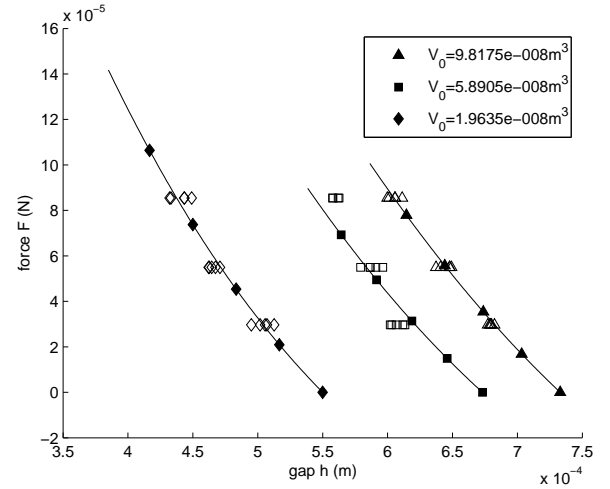


Fig. 11. Experimental validation of the vertical force model. The unfilled symbols represent the measurements, the filled symbols on curves represent the solution from the model corresponding to the experimental setup conditions (absolute gap values depend on initial bubble size). The mean stiffness is  $0.86\text{Nm}^{-1}$  ( $\diamond$ ),  $0.67\text{Nm}^{-1}$  ( $\square$ ) and  $0.69\text{Nm}^{-1}$  ( $\triangle$ )

actuators. So far, we have validated the general concept and the model giving the stiffness of the table. There is still work to do to validate the other dynamic parameters.

The lateral stiffness of a bubble must also be studied in order to predict the lateral forces that can be handled by the device. If the stiffness is too weak for the application, it is possible to add bubbles in the system to push against the lateral faces of the table. Some technological issues must also be addressed. For example, we suppose in our model that the number of gas mole is constant. The model is very sensitive to this parameter and any gas dissolution in the liquid or any gas leak should be carefully avoided. The improvement of the anchoring sites must also be addressed using new manufacturing technologies.

Finally, the current prototype is actuated manually by an operator. An new actuation system, which can be driven by a controller, is currently under development.

### ACKNOWLEDGMENT

The authors would like to thank the BRIC from Université libre de Bruxelles and PHC-Tournesol funding (WBI-FNRS) for their financial support.

### REFERENCES

- [1] Vladimir S. Ajaev, G. M. Homsy, and S. J. S. Morris. Dynamic response of geometrically constrained vapor bubbles. *J. Colloid Interface Sci.*, 254:346–354, 2002.
- [2] H. Bouazaze, S. Cattarin, F. Huet, M. Musiani, and R.P. Nogueira. Electrochemical noise study of the effect of electrode surface wetting on the evolution of electrolytic hydrogen bubbles. *J. Electroanalytical Chemistry*, 597:60–68, 2006.
- [3] Sang Kug Chung, Yuejun Zhao, and Sung Kwon Cho. On-chip creation and elimination of microbubbles for a micro-object manipulator. *J. Micromech. Microeng.*, 18(9):095009 (13pp), 2008.
- [4] Cédric Clévy, Arnaud Hubert, and Nicolas Chaillet. Flexible micro-assembly system equipped with an automated tool changer. *J. Micro-Nano Mech.*, 4(1-2):59–72, 2008.
- [5] Ron Darby and M. S. Haque. The dynamics of electrolytic hydrogen bubble evolution. *Chem. Eng. Sci.*, 28:1129–1138, 1973.
- [6] Nikolai Dechev, William L. Cleghorn, and James K. Mills. Microassembly of 3-d microstructures using a compliant, passive microgripper. *J. Microelectromechanical Syst.*, 13(2):176–189, 2004.

- [7] Peigang Deng, Yi-Kuen Lee, and Ping Cheng. The growth and collapse of a micro-bubble under pulse heating. *International Journal of Heat and Mass Transfer*, 46:4041–4050, 2003.
- [8] Peigang Deng, Yi-Kuen Lee, and Ping Cheng. An experimental study of heater size effect on micro bubble generation. *International Journal of Heat and Mass Transfer*, 49:2535–2544, 2006.
- [9] John Evans and Marina Del Rey. Apparatus and method for regulating fluid flow with a micro-electro mechanical block, 2001. US Patent 6283440.
- [10] M. Gauthier, S. Régnier, P. Rougeot, and N. Chaillet. Analysis of forces for micromanipulations in dry an liquid media. *Journal of Micromechatronics*, 3:389–413, 2006.
- [11] Pierre Lambert. *Capillary Forces in Microassembly: Modeling, Simulation, Experiments, and Case Study*. Microtechnology and MEMS. Springer, October 2007.
- [12] Dmitri Lapotko and Ekaterina Lukianova. Laser-induced micro-bubbles in cells. *International Journal of Heat and Mass Transfer*, 48:227–234, 2005.
- [13] S. Lee, W. Sutomo, C. Liu, and E. Loth. Micro-fabricated electrolytic micro-bubblers. *International Journal of Multiphase Flow*, 31:706–722, 2005.
- [14] Cyrille Lenders, Michaël Gauthier, and Pierre Lambert. Meniscus-supported compliant table, 2009. patent request submitted: EP 09 172715.
- [15] Cyrille Lenders, Michaël Gauthier, and Pierre Lambert. Microbubble generation using a syringe pump. In *Proceedings of the 2009 IEEE International Conference on Intelligent Robots and Systems*, Saint-Louis (Missouri), October 11-15 2009.
- [16] Steven Lubetkin. The motion of electrolytic gas bubbles near electrodes. *Electrochimica Acta*, 48:357–375, 2002.
- [17] M. Mastrangeli, S. Abbasi, C. Varel, C. Van Hoof, J.-P. Celis, and K.F. Bohringer. Self-assembly from milli- to nanoscales: methods and applications. *J. Micromech. Microeng.*, 19, 2009.
- [18] Abhijit Mukherjee and Satish G. Kandlikar. Numerical simulation of growth of a vapor bubble during flow boiling of water in a microchannel. *Microfluid Nanofluid*, (1):137–145, 2005.
- [19] Alexandros Papavasiliou, Albert Pisano, Dorian Liepmann, and John Evans. Controlling physical motion with electrolytically formed bubbles, 2001. Patent: WO0194823.
- [20] Dan O. Popa and Harry E. Stephanou. Micro and meso scale robotic assembly. In *WTEC Workshop: Review of U.S. Research in Robotics*. WTEC, 2004.
- [21] Y. Tian, B. Shirinzadeh, D. Zhang, X. Liu, and D. Chetwyn. Design and forward kinematics of the compliant micro-manipulator with lever mechanisms. *Precis. Eng.*, 33:466–475, 2009.
- [22] A. Volanschi, W. Olthuis, and P. Bergveld. Gas bubbles electrolytically generated at microcavity electrodes used for the measurement of the dynamic surface tension in liquids. *Sens. Actuators, A*, 52:18–22, 1996.
- [23] Mohd Nashrul Mohd Zubir, Bijan Shirinzadeh, and Yanling Tian. Development of a novel flexure-based microgripper for high precision micro-object manipulation. *Sens. Actuators, A*, 150:257–266, 2009.